THE ASTROPHYSICAL JOURNAL, 493:793–802, 1998 February 1

SIMULATED INFRARED EMISSION SPECTRA OF HIGHLY EXCITED POLYATOMIC MOLECULES: A DETAILED MODEL OF THE PAH-UIR HYPOTHESIS

D. J. COOK[1] AND R. J. SAYKALLY[2]
Department of Chemistry, University of California, Berkeley, CA, 94720-1460
Received 1997 June 26; accepted 1997 September 4

ABSTRACT

A detailed description of the polycyclic aromatic hydrocarbon (PAH)/unidentified infrared band (UIR) mechanism is presented in which experimental spectral bandshape functions are used to simulate IR emission spectra for individual molecules. These spectra are additively superimposed to produce a conglomerate spectrum representative of a family of PAH molecules. Ab initio vibrational frequencies and intensities for nine PAHs (neutral and cationic) as large as ovalene are used in conjunction with measured bandshape and temperature-dependent redshift data to simulate the UIR bands. The calculated spectra of cations provide a closer match to the UIRs than do those of the neutrals. However, the PAH cations used in the simulations fail to reproduce the details of the UIR emission spectra. The discrepancies are potentially alleviated if both larger PAHs and a greater number of PAHs were included in the simulation.

Subject headings: infrared: ISM: lines and bands — ISM: molecules — molecular data — molecular processes — planetary nebulae: general — radiation mechanisms: nonthermal

1. INTRODUCTION

The interstellar unidentified infrared bands (UIRs) are observed in emission toward sources in which interstellar dust is irradiated with UV light. Polycyclic aromatic hydrocarbons (PAHs) have received much attention as potential carriers of the UIRs (Allamandola et al. 1995; Allamandola, Tielens & Barker 1985, 1989b; Léger & d'Hendecourt 1989; Léger & Puget 1984). In the PAH model of the UIRs, a PAH molecule absorbs a UV photon, rapid internal conversion to the ground electronic state follows, and the energy of the UV photon is distributed randomly among the vibrational modes of the PAH. The PAH then cools by IR emission, thereby generating the UIRs. To assess the feasibility of the PAH-UIR hypothesis, several models have been presented in the literature in which the anticipated emission from PAHs is compared to the UIRs (Allamandola et al. 1989a; Schutte, Tielens & Allamandola 1993). Because of the previous dearth of information regarding the spectra of gaseous PAHs obtained under conditions of high internal excitation, previous models have not considered the process by which bands with finite bandwidth at differing frequencies combine to produce a conglomerate spectrum.

The PAH-UIR hypothesis can be directly tested by experiment if IR emission is observed from isolated, gas phase PAHs following UV excitation. Experiments which have taken this direct approach are typically hindered by a combination of low signal and high blackbody background, which limits the results to observation of the 3.3 μm C—H stretch (Brenner & Barker 1992; Cherchneff & Barker 1989; Cook et al. 1997; Schlemmer et al. 1994; Shan, Suto & Lee 1991; Williams & Leone 1995). These experiments did demonstrate that the UV absorption-internal conversion-IR emission mechanism is quite general for small PAHs. The remaining problem is to demonstrate that emission from a population of PAHs and/or PAH cations does indeed reproduce the detailed spectral features—frequencies, bandshapes, and relative intensities—of the UIRs. Alternative experimental approaches that allow observation of the entire portion of the IR spectrum relevant to the UIRs include UV laser induced desorption (UV-LID) (Cook et al. 1997, 1996; Schlemmer et al. 1994), and observation of IR emission and absorption from PAHs a high temperature cell in thermal equilibrium (Joblin et al. 1995, 1994). While these experiments have provided characteristic spectral parameters for highly excited PAHs, the spectra of the individual small, neutral PAHs explicitly studied differ greatly from the UIRs.

Experimental measurement of gas phase emission from the types of PAHs which are anticipated to survive in the harsh conditions of the interstellar environment currently eludes experiment. In many UIR sources (planetary nebulae and the Orion Nebula are examples) the UIR emission is observed on the H I side of an H I/H II interface, and the UIR carriers are irradiated with photon energies up to the 13.6 eV cutoff. In the context of the PAH-UIR hypothesis, these photon energies lead to a PAH population that is both largely ionized and which is robust with respect to unimolecular dissociation. Models of interstellar PAH photochemistry (Allain, Leach, & Sedlmayr 1996a, 1996b), which take into account the results of PAH photolysis experiments using synchrotron radiation (Jochims et al. 1994), indicate that PAH cations with fewer than 50 carbon atoms ($N_C < 50$) are not anticipated to be stable in regions associated with UIR generation.

In the absence of experimental emission spectra from the PAH cations, absorption data from matrix isolation experiments and the results of ab initio calculations become the sole sources of IR spectral data. These experiments and calculations clearly demonstrate that the cations provide a better match to the UIR spectra than do the neutrals. However, these methods only provide spectroscopic data for molecules under low temperature conditions. In the present paper, spectroscopic parameters from neutral PAH

[1] Department of Chemistry, University of Pennsylvania, Philadelphia, PA, 19104-6323.
[2] To whom correspondence should be addressed.

gas phase emission experiments performed at high excitation energy over the entire range of the UIR bands are combined with the results of ab initio calculations to provide model PAH emission spectra for PAH cations for which ab initio data currently exists. Although the currently available data do not include PAH cations with $N_C > 50$, the methods presented here can be applied to such cations when the rapidly advancing field of quantum chemistry provides data for them.

2. THE UIR EMISSION MECHANISM

2.1. *Density of States, Anharmonicity, and Sequence Bands*

The effects of high vibrational excitation are revealed by the PAH emission experiments. Spectra obtained in such experiments consistently exhibit an increasing redshift of the bands and greater broadening with increasing internal excitation (Cook et al. 1997; Joblin et al. 1995; Schlemmer et al. 1994; Williams & Leone 1995). The PAHs studied in these experiments are excited with multiple quanta in the various vibrational modes. When a single quantum transition is observed in a particular mode, excitation in modes other than the mode of interest leads to intermode anharmonicity. Each way of partitioning the energy into the vibrational modes constitutes a different state, with a unique frequency for a single quantum transition in a particular mode.

Herzberg has addressed the case in which the density of states, $\rho(E)$, is small. In such a case, if a single quantum transition is observed in a high-frequency mode, a progression of sequence bands arising from discrete vibrational transitions associated with increasing quanta in a low-frequency mode can be observed (Herzberg 1968). Under both the conditions of UIR generation and the laboratory experiments, the density of states rapidly becomes large, as is illustrated in Figure 1. Such a high density of states generates a multitude of sequence bands which are blended into an unresolvable continuum. Because anharmonicity produces a redshift of the vibrational bands, the trend of increasing redshift and band broadening can be understood, given knowledge of this property.

2.2. *Population of Excited PAH Vibrational States*

The construction of additive bandshapes from a population of individual molecules in a molecular model of UIR emission requires a detailed examination of the problem; this discussion follows the previous work of Schutte et al. (1993) and Allamandola et al. (1989b). When the energy deposited by a single photon excitation is considered, the internal energy in a PAH following the UV absorption-internal conversion mechanism is described by a microcanonical ensemble. The probability of finding one or more quanta in any particular normal mode can be determined if the density of states is known. If $P(E, i, v)$ is defined as the probability of populating mode i with v quanta at an energy E, then

$$P(E, i, v) = g(i, v)\,\frac{\rho_r(E - vhv_i)}{\rho(E)}\,. \tag{1}$$

In equation (1), $\rho_r(E - vhv_i)$ is the density of states remaining after the energy is partitioned into the vth level of mode i; this is determined through a separate calculation of the density of states which excludes mode i. The quantity $g(i, v)$ is the degeneracy of the vth level of mode i. If mode i is an m-fold degenerate normal mode, then $g(i, v)$ is given by

$$g(i, v) = \frac{(v + m_i - 1)!}{(m_i - 1)!v!}\,. \tag{2}$$

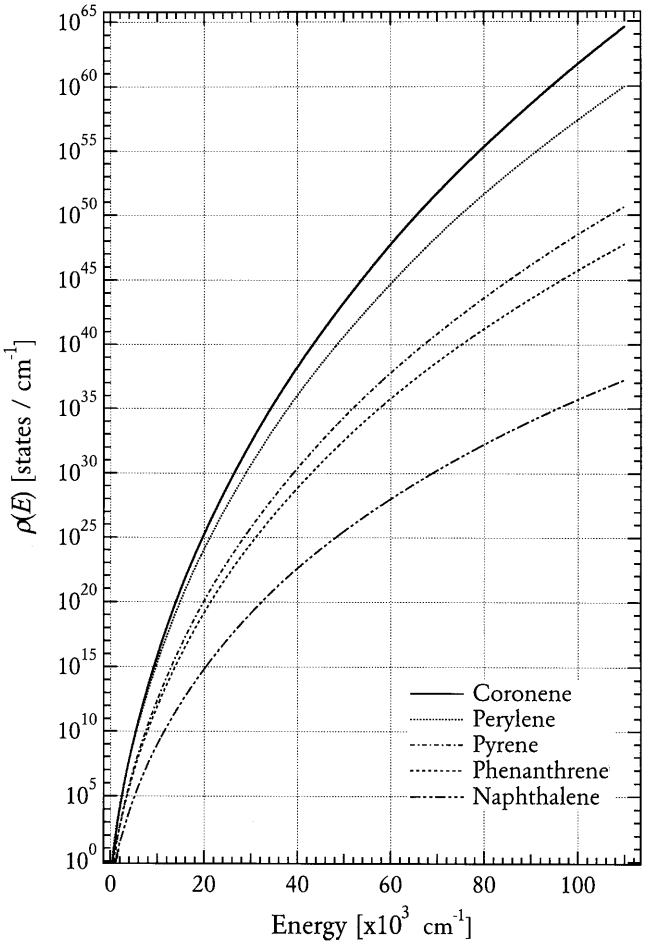

FIG. 1.—PAH density of states [$\rho(E)$] using the Beyer-Swinehart algorithm (Beyer & Swinehart 1973; Stein & Rabinovitch 1973) for harmonic oscillators with a grain size of 1 cm^{-1}. Normal mode frequencies are from ab initio data (Langhoff 1995, private communication; Langhoff 1996).

A canonical ensemble can be used to approximate the results of a microcanonical ensemble. In the thermal approximation, the probability finding of v quanta in mode i has the following familiar form:

$$P(T, i, v) = g(i, v)q_i^{-1}\,\exp\left(\frac{-vhv_i}{kT}\right). \tag{3}$$

For an m-fold degenerate normal mode,

$$q = \left[1 - \exp\left(\frac{-vhv_i}{kT}\right)\right]^{-m_i}. \tag{4}$$

The effective temperature of a microcanonical ensemble with energy E_{MC} is given by the temperature at which

$$\langle E(T)\rangle = E_{MC}\,. \tag{5}$$

This effective temperature can be determined from the vibrational heat capacity;

$$\langle E(T)\rangle = \sum_{i=1}^{s} m_i hv_i\left[\exp\left(\frac{hv_i}{kT}\right) - 1\right]^{-1}. \tag{6}$$

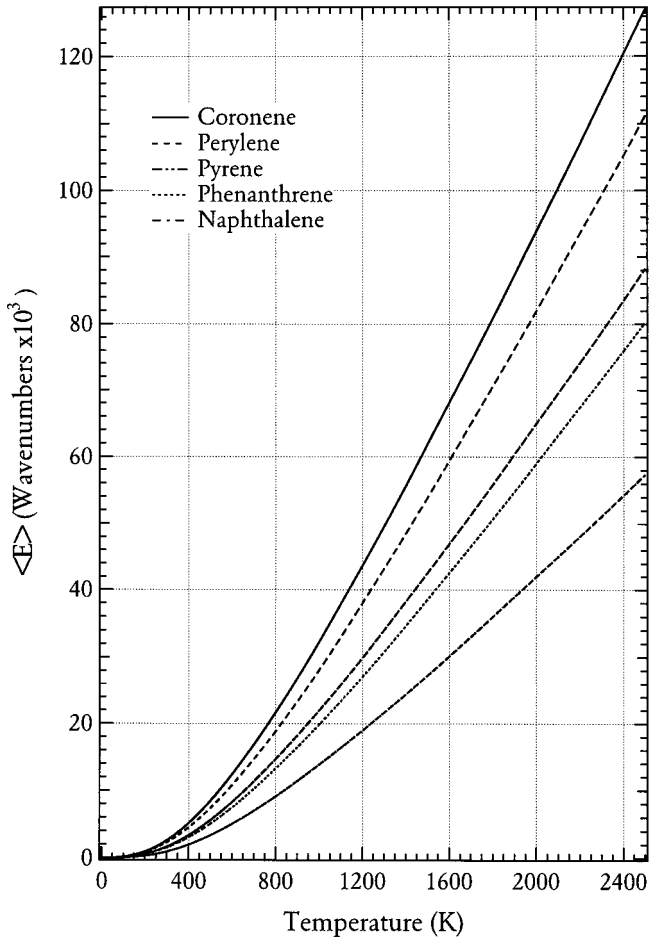

FIG. 2.—PAH vibrational heat capacities, calculated assuming harmonic oscillators and using ab initio frequencies from Langhoff (1996).

Vibrational heat capacities for several small PAHs are displayed in Figure 2.

For a thermal ensemble, different molecules have different internal energies. As pointed out by Allamandola et al. when properties with a strong nonlinear dependence on E, such as the rate of unimolecular decomposition, are considered, the thermal ensemble differs considerably from the microcanonical ensemble. However, if emission rates from high-energy molecules in a thermal ensemble are averaged with rates from low-energy molecules, the result can be similar to that calculated from a microcanonical distribution of $E_{\rm MC} = \langle E(T) \rangle$. Schutte et al. have investigated different methods of approximating PAH emission spectra and find that the thermal approximation is often suitable for modeling PAH emission data.

2.3. *Emission from a Mode in an Excited Polyatomic Molecule*

First, the intensity produced by emission from a two-state system will be considered. Since there is no apparent rotational structure in the UIRs, the emission spectrum will be discussed in terms of vibrational transitions. For a diatomic molecule, the total photon flux arising from a transition from an upper state (v') to a lower state (v'') is determined by the Einstein coefficient for the transition and the population of the upper state;

$$\Phi_{q,v'} = N_{v'} A^{v'' \leftarrow v'} . \tag{7}$$

(The conventions of radiometric nomenclature are followed: the subscript q is used to denote quantities with dimensions of photons and the subscript e is used to denote quantities with dimensions of power.) Under the harmonic oscillator approximation, the Einstein coefficient for emission from higher quantum states is directly proportional to the intensity of the $0 \leftarrow 1$ transition,

$$A^{v'' \leftarrow v'} = v' A^{0 \leftarrow 1} . \tag{8}$$

When emission from highly excited molecules is observed, intermode anharmonicity typically prevents the observation of discrete bands. Therefore, all possible transitions of the following type contribute to emission observed in a band:

$$\Delta v_{j=i} = 1 \quad \text{and} \quad \Delta v_{j \neq i} = 0 . \tag{9}$$

Equation (8) can be applied to polyatomic molecules. If both intramode and intermode anharmonicity are ignored,

$$\Phi_{q,i,v} = NP(E, i, v) v A_i , \tag{10}$$

where $A_i = A_i^{0 \leftarrow 1}$, and $v = v'$ since only single quantum transitions are considered. This also takes advantage of the relationship between the upper state population and the total number of molecules; $N_{v'} = NP(v')$.

Since all states with $v_i > 0$ contribute to the emission observed in a band, the flux is given by the following sum:

$$\Phi_{q,i} = \sum_{v=1}^{\infty} NP(E, i, v) v A_i . \tag{11}$$

If $P(T, i, v)$ is used to approximate $P(E, i, v)$, this converges to a simple result,

$$\Phi_{q,i} = N \left[\exp\left(\frac{h\nu_i}{kT} \right) - 1 \right]^{-1} A_i . \tag{12}$$

This result applies to both degenerate and nondegenerate modes.

2.4. *The Radiative Cascade*

Photon energies in typical UIR sources can exceed 100,000 $\rm cm^{-1}$. Emission of a 1000 $\rm cm^{-1}$ photon corresponds to only $\approx$0.1% of the maximum available UV energy. Therefore, the total emitted flux following absorption of a UV photon includes the sum of the flux emitted as the molecule cools via a radiative cascade process. A detailed model of the UIR emission should include this radiative cascade. Models of UIR emission which include the radiative cascade have been presented by Schutte et al. (1993) and also by Allamandola et al. (1989b).

The molecular energy loss at time t is equal to the sum of the power emitted by each band and depends on the energy at time t;

$$\frac{dE}{dt} = - \sum_{j=1}^{s} \Phi_{e,j}(E) . \tag{13}$$

The energy at time t can therefore be determined by the recursive relationship,

$$E(t, E_{\rm UV}) = E_{\rm UV} - \int_0^t \sum_{j=1}^{s} \Phi_{e,j}[E(t')] dt' . \tag{14}$$

This can be solved numerically by using a discrete representation for time and evaluating the energy at time $t + \delta t$ using the energy and radiative power at time t. These

relationships assume the PAHs absorb no energy from the background blackbody radiation field, which is typically ≈ 100 K. At some time (t_f) the internal energy in the molecule will decay to the background thermal value and the radiative cascade can be considered complete. The total number of IR photons emitted by mode i following absorption of a UV photon is then given by

$$N_{q,i}(E_{\rm UV}) = NA_i \int_0^{t_f} \left\{ \sum_{v=1}^{\infty} vP[E(t, E_{\rm UV}), i, v] \right\} dt \ . \quad (15)$$

The time averaged photon flux emitted into the band arising from mode i is the product of the number of photons given by the preceding result and f_λ, the molecular absorption rate of UV photons at wavelength λ

$$\bar{\Phi}_{q,i}(E_{\rm UV}) = f_\lambda N_{q,i}(E_{\rm UV}) \ . \quad (16)$$

So far, only single UV photon energies have been considered. Under interstellar conditions, the radiation which excites the PAHs consists of a broad blackbody continuum which originates in the photosphere of a nearby star. Neglecting photoionization, the photon wavelengths which must be considered range from the 91 nm (110,000 $\rm cm^{-1}$) H I ionization threshold ($\lambda_{\rm min}$) to the long wavelength cutoff of the PAH absorption spectrum ($\lambda_{\rm max}$). For the large PAH cations which are the most viable UIR candidates, this long-wavelength cutoff will typically extend into the visible.

At modest energies above the threshold for excitation to the upper state, the large density of states and rapid upper state dynamics, such as internal conversion, will lead to a broad absorption continuum even under isolated conditions. Therefore, the UV spectra of PAHs typically consist of very broad absorption bands; these very broad bands are better described by empirical wavelength dependent absorption cross sections than by Einstein coefficients. If the absorption cross section is known, the molecular photon absorption rate per unit UV wavelength is simply

$$f_\lambda(\lambda) = \sigma(\lambda)\mathscr{E}_{q,\lambda}(\lambda) \ , \quad (17)$$

where $\mathscr{E}_{q,\lambda}(\lambda)$ has dimensions of (photons)/(area $\times$ time $\times$ wavelength). The photon flux emitted into the band is now the integral of time averaged photon flux per unit UV wavelength,

$$\langle \Phi_{q,i} \rangle = \int_{\lambda_{\rm min}}^{\lambda_{\rm max}} f_\lambda(\lambda) N_{q,i}(hc\lambda^{-1}) d\lambda \ . \quad (18)$$

2.5. *IR Emission Spectra from a Single PAH and a Collection of PAHs*

The emission spectrum resulting from a transition is described by a spectral radiometric quantity ($\Phi_{q,\xi}$), which is the product of the bandshape function [$g_\xi(\xi)$] and the total flux (Φ_q); ξ is the independent spectral variable, and can take the form of frequency or wavelength. Therefore, the wavelength dependent spectrum for a single mode (i) is described as

$$\Phi_{q,v,i}(v) = g_{v,i}(v - v_i)\Phi_{q,i} \ . \quad (19)$$

The spectral emission from a molecule is given by the sum of the emission from the different modes

$$\Phi_{q,v}(v) = \sum_{i=1}^{s} \Phi_{q,v,i}(v) \ . \quad (20)$$

In a similar manner, the emission spectrum from a collection of M different molecules is given by the sum of spectra of the individual molecules

$$\Phi_{q,v}(v) = \sum_{n=1}^{M} \Phi_{q,v,n}(v) \ . \quad (21)$$

Therefore, if a bandshape function is known, the spectral emission from a collection of excited PAHs can be described by these last three equations. The bandshape function, in principle, depends on the molecule, the particular vibrational band, and the internal energy in the molecule. If emission from PAHs excited under laboratory conditions is monitored, these preceding equations are appropriate. If however, emission under interstellar conditions is considered, these preceding equations are not rigorous since the internal energy and thus the bandshape function change through the radiative cascade. This can be accounted for by including bandshape functions in equation (15) and results in the following equation for the spectral power radiated by a population of excited molecules under interstellar conditions:

$$\Phi_{e,v}(v) = h\nu \sum_{n=1}^{M} N_n \sum_{i=1}^{s} \quad (22)$$
$$\int_{\lambda_{n,\rm min}}^{\lambda_{n,\rm max}} \sigma_n(\lambda_{\rm UV})\mathscr{E}_{q,\lambda}(\lambda_{\rm UV}) A_{n,i} \left(\int_0^{t_f} \left\{ \sum_{v=1}^{\infty} vP\left[E\left(t, \frac{hc}{\lambda_{\rm UV}}\right), n, i, v \right] \right.\right.$$
$$\left.\left. \times g_{v,n,i}\left[v - v_{n,i}, E\left(t, \frac{hc}{\lambda_{\rm UV}}\right) \right] dt \right\} \right) .$$

3. SYNTHESIZED SPECTRA FOR NEUTRAL AND IONIZED PAHs

Schutte et al. (1993) have presented a model of the PAH-UIR emission process in which simulated spectra are presented. This model is based upon a detailed analysis of the known PAH photophysics and includes the effects of the radiative cascade, an extremely broad PAH size range ($N_{\rm C} = 14$ to $N_{\rm C} \gg 1000$), anticipated changes in spectral parameters due to dehydrogenation, the anticipated UV absorption cross sections, and differences in the UV blackbody continuum between different sources. Because this model included such a broad PAH size distribution, certain approximations were necessary. The long wavelength UV absorption cross section was assumed to scale with $N_{\rm C}$. The cross section short of $\lambda_{\rm max}$ was also assumed to be wavelength independent, scale with $N_{\rm C}$, and $\sigma/N_{\rm C}$ was assumed to be nearly constant. Only neutral PAHs were considered for this analysis.

Similar approximations regarding the IR spectral properties were also necessary. Einstein A coefficients corresponding to C—H stretching, and C—H in and out of plane bending were assumed to scale with $N_{\rm H}$; C—C stretching cross sections were assumed to scale with $N_{\rm C}$. The frequencies for these transitions were assumed to be equal, so that the intensities in these bands from different modes and different PAHs would be additive. These frequencies were also assumed to occur at the UIR frequencies thought to correspond to the particular type of vibration. The contributions from the bandshapes of the individual modes were also not considered.

Therefore, the model of Schutte et al. assumes that a large population of PAHs will generate bands at frequencies cor-

responding to the UIRs. Rather than addressing whether a population of PAHs can reproduce the detailed UIR spectra, their model addresses problems concerning the relative intensity of the bands and shows how different portions of the PAH size distribution can contribute to the different bands. For example, this model anticipates that the 3.3 μm band originates primarily from PAHs with $N_C < 80$ and shows PAHs with $N_C \geq 80$ can contribute significantly to, and actually dominate, the emission from the other bands.

In order to generate a synthesized spectrum from a collection of PAHs, the PAH IR frequencies and bandwidths must be considered explicitly. Of course, the frequencies of the neutral PAHs which can be chemically isolated can be measured empirically. For many of these molecules, emission spectra can be measured under astrophysically relevant conditions, as has been discussed in our recent paper (Cook et al. 1997). The spectra of PAH *cations* have been measured with matrix techniques (Allamandola et al. 1995; Hudgins & Allamandola 1995a, 1995b; Hudgins, Sandford & Allamandola 1994; Szczepanski, Chapo & Vala 1993; Szczepanski et al. 1992; Szczepanski & Vala 1993a, 1993b; Szczepanski et al. 1993; Szczepanski, Wehlburg & Vala 1995; Vala et al. 1994), and the normal mode frequencies and intensities have been evaluated through ab initio calculations (de Frees et al. 1993; Langhoff 1996; Pauzat et al. 1992; Szczepanski et al. 1993; Vala et al. 1994). The purpose of the remainder of this report will be to generate simulated spectra based on the ab initio calculations and empirically measured spectral parameters from high-temperature emission data. Because the matrix data do not include bands which are obscured by neutral species also present in the matrix, the ab initio data, which provide the *complete* set of IR active transitions are used instead.

The ab initio calculations of Langhoff provide a convenient set of normal mode frequencies and intensities for several neutral and ionized PAHs. Included along with the report (Langhoff 1996) of the ab initio calculations is a comparison between a conglomerate stick spectrum (simply using the calculated bandstrengths in km mol^{-1}) from several PAH cations and the spectrum of the Orion Bar. A realistic model of the PAH emission spectrum using this ab initio data and including the effects of high internal energy is therefore of substantial interest.

The first problem is to consider the amount of detail to place in the model. In order to simulate the conglomerate spectrum, the bandshape functions need to be included for every normal mode. If accurate relative intensities are desired, the upper state populations resulting from the radiative cascade and UV excitation must be considered. However, the PAHs considered explicitly here are somewhat small for the PAH-UIR hypothesis. Absorption of photons with energies as high as 100,000 cm^{-1} dissociates the small molecules included in the model (such as pyrene and phenanthrene). The relative intensities calculated under such conditions are not anticipated to be representative of the relative intensities of the larger molecules which are acknowledged to be better candidates for UIR emission. If, on the other hand, a relatively simple thermal approximation is made for the upper state populations, the upper state populations and relative intensities for a small PAH and a large PAH at the same temperature will be similar. Because of these considerations, the emission is calculated for a collection of PAHs at a single temperature, and the spectral photon flux is described by

$$\Phi_{q,\tilde{\nu}}(\tilde{\nu}) = \sum_{n=1}^{M} N_n \sum_{i=1}^{s} g_{\tilde{\nu},n,i}(\tilde{\nu} - \tilde{\nu}_i)\left[\exp\left(\frac{hc\tilde{\nu}_{n,i}}{kT}\right) - 1\right]^{-1} A_{n,i} \,. \tag{23}$$

Since the UIR spectra are usually presented in dimensions of power per unit wavelength, rather than photons per wavenumber, the following conversion is necessary:

$$\Phi_{l,\lambda}(\lambda) = \frac{N_A hc}{M\lambda^3}\,\Phi_{q,\tilde{\nu}}(\lambda) \,. \tag{24}$$

The result now can be conveniently expressed in units of kW nm^{-1} (mole of sample)$^{-1}$. An equal mole fraction of each molecule is assumed.

Using equations (23) and (24), the spectrum can be described with the following set of parameters: the frequencies and Einstein A coefficients for each mode of each molecule, the bandwidths for the Lorentzian bandshape functions for each mode, and the temperature. The cation and neutral ab initio frequencies and intensities for the nine PAHs listed in Figure 3 are taken from the literature (Langhoff 1996). The intensities reported in units of km mol^{-1} and were converted to Einstein A coefficients with the following relationship:

$$A = \frac{8\pi}{N_A c}\,\nu^2 S$$

$$A(\mathrm{s}^{-1}) \cong \left(1.2512 \times 10^{-7}\,\frac{\mathrm{mol\ cm}^2}{\mathrm{km\ s}}\right)\tilde{\nu}^2 S\left(\frac{\mathrm{km}}{\mathrm{mol}}\right). \tag{25}$$

An increasing redshift with vibrational temperature is an important aspect regarding the spectroscopy of PAHs with high internal energy. Since the ab initio quantities are calculated for PAHs at zero temperature, it is necessary to deter-

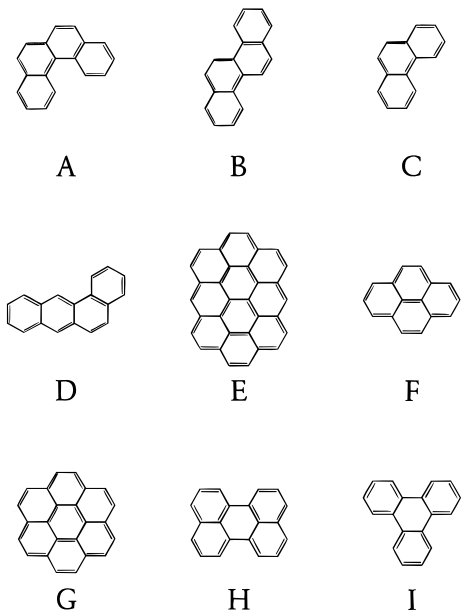

FIG. 3.—Nine PAHs with available ab initio data used for simulated emission spectra. (*a*) 3,4-benzophenanthrene, (*b*) chrysene, (*c*) phenanthrene, (*d*) benzanthracene, (*e*) ovalene, (*f*) pyrene, (*g*) coronene, (*h*) perylene, (*i*) triphenylene. Peripheral hydrogen atoms are omitted for clarity.

mine a characteristic redshift which can be applied to the calculated frequencies. This characteristic redshift can be determined by comparison of the temperature dependent redshift measurements of Joblin et al. (1995) with the ab initio data of Langhoff (1996). The redshift data reported by Joblin et al. takes the form,

$$\nu(T) = \nu_L(0) + \chi(T) \, . \tag{26}$$

This is an empirical relationship, based on measurements of bands at high temperature. It is unknown whether this relationship remains linear when extrapolated to zero temperature; therefore, $\nu_L(0)$ does not necessarily correspond to the ab initio frequency. For determination of the temperature-dependent redshift when starting with an ab initio frequency (ν_0) the following relationship,

$$\nu(T) = \nu_0 + \Delta\nu_{\rm RS} + \chi(T) \, , \tag{27}$$

where

$$\Delta\nu_{\rm RS} = \nu_L(0) - \nu_0 \, , \tag{28}$$

should be used. $\Delta\nu_{\rm RS}$ can be considered to be an empirical shift between the extrapolated zero K value from high-temperature emission experiments and the ab initio frequency. For naphthalene and ovalene, Joblin and co-workers provided redshift data for only the 3.3 μm band. More extensive data was provided for bands arising from pyrene and coronene. Values of $\chi(T)$ and $\Delta\nu_{\rm RS}$ are presented in Table 1 for the individual bands and the mean values. The redshift data are grouped into different PAH spectral regions.

The 3.3 μm bands are the result of multiple normal modes. Therefore, for the purpose of comparison, an effective ab initio frequency must be determined. For these modes, an effective frequency is determined using a weighted average,

$$\langle \nu \rangle = \left(\sum_{i=1}^{s} A_i \right)^{-1} \sum_{i=1}^{s} A_i \nu_i \, . \tag{29}$$

Characteristic Lorentzian bandwidths for these transitions have been obtained from the parameters from the UV-LID SPIRES experiments described elsewhere (Cook et al. 1997). The two largest PAHs studied, perylene and coronene, are thought to be more representative of the UIR carriers. These molecules consistently exhibit bandwidths which are smaller than or equal to the UIR bandwidths. On the other hand, the complete ensemble of PAHs studied by the UV-LID technique produce average bandwidths greater than the bandwidths of the corresponding UIR bands; any model which uses these parameters can never faithfully reproduce the observed UIR spectra. Therefore, the average individual bandwidths for perylene and coronene are used to model the UIR spectra in the present study.

The 3.3 μm band is consistently observed for every PAH studied and also appears in the ab initio calculations with a similar regularity. Since the temperature-dependent redshift is incorporated into the model, an effective temperature can be determined by fitting the calculated 3.3 μm band to a UIR band at 3.3 μm. The spectrum of NGC 7027 was used to determine the temperature (Roche et al. 1996). A slightly modified version of equation (27) was used to fit the temperature, using data for the nine neutral PAHs listed in

TABLE 1

PAH Temperature-dependent Redshifts

Molecule	$\chi(T)$[a] ($\times 10^{-2}$ cm^{-1} K^{-1})	$\nu_L(0)$[a] (cm^{-1})	ν_0[b] (cm^{-1})	$\Delta\nu_{\rm RS}$[c] (cm^{-1})
C—H Stretch				
Naphthalene.....	−2.01[d]	3074.7	3067.6	7.1
Pyrene	−2.22	3062.9	3066.5	−3.6
Coronene	−3.52	3077.2	3063.7	13.5
Ovalene	−4.90	3082.3	3063.2	19.1
Mean.....	−3.55	...	...	9.0
C—C Stretch				
Coronene 6.2 mm.....	−4.36	1635.1	1602.7	32.4
Coronene 7.7 μm	−2.38	1325.9	1312.4	13.5
Mean.....	−3.37	...	...	23.0
C—H In-Plane Bend				
Pyrene	1.00	1187.9	1188.3	−0.4
Coronene	0.840	1141.5	1140.3	1.2
Mean.....	0.92	...	...	0.5
C—H Out-of-Plane Bend				
Pyrene	−1.69	847.6	848.3	−0.7
Coronene	−2.30	865.0	864.4	0.6
Mean.....	−2.00	...	...	0

[a] Using calculations with band positions determined by the midpoint at half maximum. Experiment (Joblin et al. 1995).

[b] Effective 3.3 μm ab initio frequencies were determined using eq. 3539 (Langhoff 1996).

[c] Rounded to the nearest 0.5.

[d] A trend arises when the 3.3 μm bands are examined; $\chi(T)$ increases with increasing PAH size. Because the interest is on obtaining parameters for larger PAHs, naphthalene was excluded from the determination of the mean value of $\chi(T)$.

Figure 3,

$$\Phi_{l,\tilde{\nu}}(\tilde{\nu}) = Chc\tilde{\nu}\Phi_{q,\tilde{\nu}}(\tilde{\nu}) . \quad (30)$$

Value C is an arbitrary multiplicative constant, and $\Phi_{q,\tilde{\nu}}(\lambda)$ is determined from equation (23). The two free parameters are C and T. The results of this fit are displayed in Figure 4. A temperature of 1022 K is obtained with a 95% confidence interval of ± 7.7 K. Because it is not known how closely the temperature-dependent redshift of the calculated spectrum matches the actual redshift of the PAHs thought to generate the UIR band, the confidence interval merely describes the ability of the model to fit the data, rather than an actual uncertainty of the temperature of the carriers of this UIR band. From Figure 2, this temperature corresponds to 33,400 cm^{-1} of energy in coronene. If larger molecules are considered, the energy per degree of freedom can be assumed to be relatively constant. Coronene has 102 vibrational degrees of freedom, which gives 327.4 cm^{-1} per degree of freedom. A larger and potentially more relevant PAH such as $C_{66}H_{22}$ would have 258 degrees of freedom and approximately 84,000 cm^{-1} of internal energy. Therefore, the amount of vibrational excitation in these molecules if a constant temperature of 1022 K is assumed appears to be relevant to the PAH-UIR problem.

The calculated spectra for neutral and ionized PAHs which use equations (23) and (24) along with the parameters—intensities, temperature-dependent frequencies, bandwidths, and temperature—which have now been discussed are displayed in Figure 5. In the interstellar environment, larger PAHs with lower effective temperatures would be expected to contribute to the lower frequency transitions. In addition, the radiative cascade would lead to a lower temperature contribution to the emission which is not considered in the model. Therefore, it is also interesting to consider the spectrum generated when temperatures of 500 and 300 K are used; these are displayed in Figures 6 and 7.

For both the neutrals and cations, none of these temperatures reproduces the UIR intensities particularly well. At 1022 K, the calculated spectrum for the neutrals is dominated by the 3.3 μm C—H stretching band. Next in intensity are the C—C stretching bands (6 to 8 μm), which are in turn much greater in intensity than are the C—H bending bands (11 to 15 μm). For the neutral PAHs, the relative intensity of the calculated C—H stretching band remains much larger than the corresponding UIR band when the lower T spectra are examined. In the case of the cations at 1022 K, the C—C stretching bands are the strongest. However the calculated relative intensity for the 3.3 μm band is still too high when compared to the UIRs. At 500 K, the relative intensity of the C—H stretching band is greatly reduced and the relative intensity of the C—H stretching transition is smaller than the comparable UIR band. At 300 K, the relative intensity of the C—H bending bands is strong when compared to the UIRs.

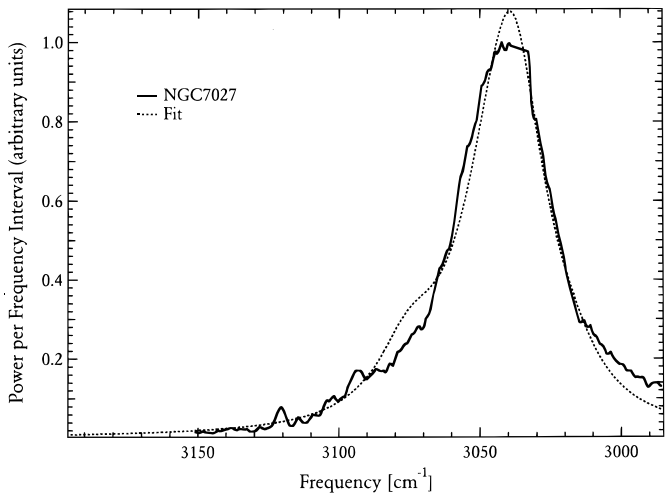

FIG. 4.—Determination of temperature for modeled emission spectra from fit of eq. (30) to UIR data. The NGC 7027 spectrum is from Roche et al. (1996). Results of fit: $T = 1022 \pm 7.7$ K; $C = 0.66 \pm 0.02$.

Since a rigorous model of the UIRs would include contributions from PAHs of different sizes and different temperatures, discrepancies in relative intensity between calculated and UIR spectra involving of bands in different parts of the spectrum are not especially significant. Consider the relative intensity of the cation C—H stretch; it is low when compared to the UIRs at 500 K and high when compared to the UIRs at 1022 K. A more detailed model could certainly reproduce the C—H stretch to C—C stretch UIR intensity ratios if the radiative cascade were considered and the proper PAH size distribution were used.

However, discrepancies involving relative intensities for bands close in frequency are not easily explained even if a multiple temperature distribution is considered. For example, the relative intensities of the solo and duo C—H OOP bending bands for the neutrals are strong when compared to the bands for the trios. However, this trend appears to be reversed in the calculated spectrum of the PAH cations.

In determining the ability of the calculated spectra to reproduce the detailed features of the UIRs, the 500 K spectra might actually be more relevant because the longer wavelengths are expected to be dominated by emission from cooler PAHs. The neutrals come closer to reproducing the 11.2 μm band; however the neutral spectrum is still dominated by a strong peak which is outside the envelope of the 11.2 μm UIR band. In the 6–9 μm region, a strong peak is observed in the neutral spectrum at 6.2 μm which is very similar to the corresponding UIR band. A similar peak appears in the cation spectrum; however, it is shifted red of the 6.2 μm UIR band. The cations come closer to reproducing the broad 7.7 μm feature than do the neutrals, but the shape of the 7.7 μm feature is not reproduced. In both the neutral and cation spectra, a strong peak is observed slightly blue of 7.0 μm, in between the 6.2 and 7.7 μm UIR peaks.

In order to reproduce the narrow 6.2 and 11.2 μm UIR bands, the carriers must consistently exhibit bands at these positions with a consistency similar to that which is observed with the 3.3 μm emission. In addition, the carriers of the UIRs must, in general, exhibit an absence of strong bands in the gap between the 6.2 and 7.7 μm UIR features. The PAHs used in these model spectra simply do not meet these criteria; hence they do not reproduce the details of the UIR spectra. The auto soot Raman spectrum of Allamandola et al. (1985) does a far better job of reproducing the details of the UIRs between 5 and 10 μm. However, it should be noted that the simulated spectra reported here only included data for nine PAHs, all of which are probably too small to survive in the UV radiation fields typically associated with UIR generation. Therefore,

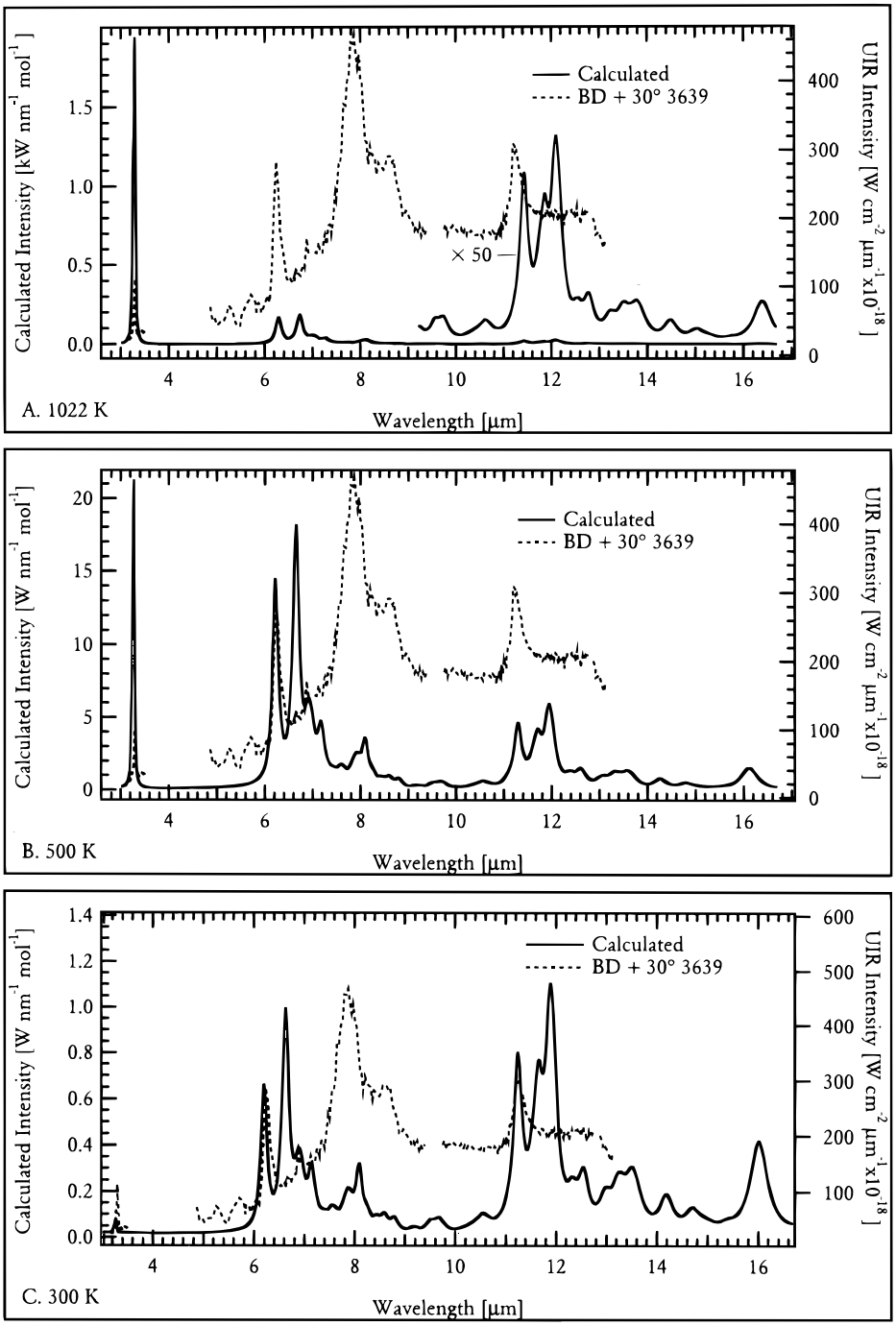

FIG. 5.—Calculated spectra for neutral PAHs at. (*a*) 1022 K, (*b*) 500 K, and (*c*) 300 K. The calculations include equal contributions from the nine PAHs depicted in Fig. 3. The BD +30° 3639 spectrum is from Allamandola et al. (1989a).

it remains to be determined whether a population of larger PAHs, which would be more relevant to the PAH-UIR hypothesis, will reproduce the details of the UIR spectra.

Although the simulated spectra presented here do not precisely reproduce the UIRs, the methods used for the simulated spectra appear to provide a promising means of testing the PAH-UIR hypothesis given a set of frequencies and intensities. If advances in theory and computational power make calculations for PAHs with $50 < N_C$ possible, these methods could help determine whether a population of larger PAHs could reproduce the UIR bands at an acceptable level of detail.

Finally, it is of interest to compare the calculated spectra of the individual neutral PAHs with the UV-LID/SPIRES spectra. These spectra are compared in Figure 7. Although it is tempting to obtain a temperature through fitting the relative intensities of the measured bands, the problems associated with obtaining accurate relative intensities make such an interpretation of questionable value.

6. CONCLUSIONS

The theoretical aspects of reproducing the UIR features by associating them with a collection of PAHs and using bandshape functions have been discussed. Experimentally obtained spectral parameters characteristic of highly excited PAHs were used to model the UIR bands. Ab initio

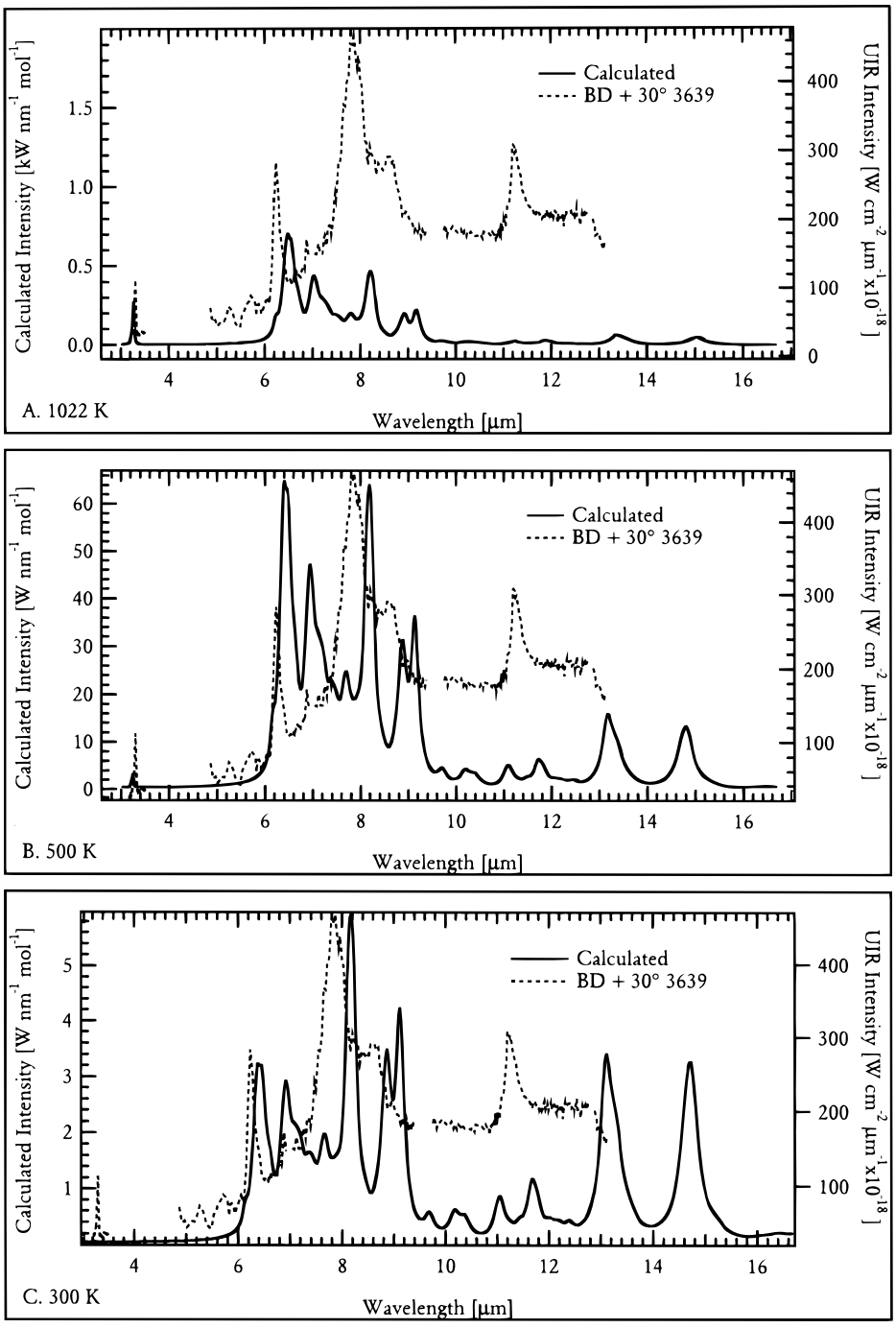

FIG. 6.—Calculated spectra for PAH cations at. (*a*) 1022 K, (*b*) 500 K, and (*c*) 300 K. The calculations include equal contributions from the nine PAHs depicted in Fig. 3. The BD +30° 3639 spectrum is from Allamandola et al. (1989a).

intensities and frequencies, and temperature-dependent redshift data from the literature, were also used as parameters for this model. The spectra for the neutral PAHs generated by the model differ substantially from the UIRs. Although the spectra calculated for the PAH cations resemble the UIRs more closely than do the neutrals, these calculated spectra still exhibit significant discrepancies from the UIR spectra. Therefore, it appears unlikely that a collection of small PAHs ($N_C \lesssim 30$) can reproduce the details of the UIR spectra. If advances in theory and computational power make the calculation of intensities and frequencies of larger PAHs (or other potential carriers, such as hydrogenated carbon clusters without the hydrogen terminated graphitic PAH structure) possible, then the methods used for these simulations could be used to assess whether a collection of larger molecules could reproduce the UIR spectra.

This work was supported by grants from the NASA Astrophysics and Exobiology Programs.

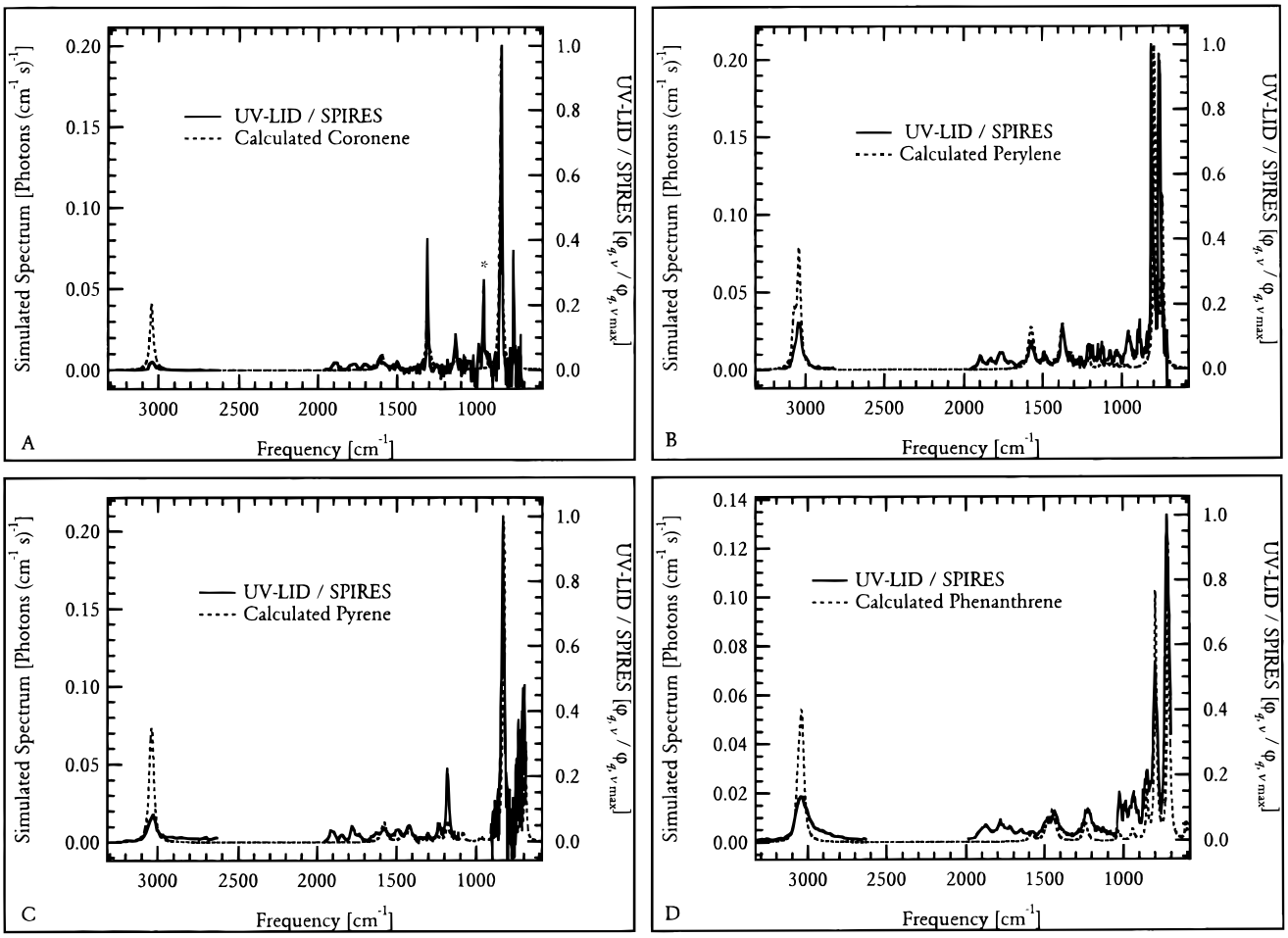

FIG. 7.—Measured and calculated spectra of the following PAHs observed with the UV-LID/SPIRES technique (Cook et al. 1997): (*a*) coronene, (*b*) perylene, (*c*) pyrene, and (*d*) phenanthrene. A temperature of 1022 K was used for the calculated spectra of all PAHs except coronene, for which a temperature of 814 K was used. The 955 cm^{-1} peak in the coronene spectrum is thought to be from either a contaminant or a photolysis product and is marked with an asterisk. A plateau which is thought to be an artifact was observed around the 1311 cm^{-1} coronene peak and has been subtracted out.

REFERENCES

Allain, T., Leach, S., & Sedlmayr, E. 1996a, A&A, 305, 602
———. 1996b, A&A, 305, 616
Allamandola, L. J., Bregman, J. D., Sandford, S. A., Tielens, A. G. G. M., Witteborn, F. C., Wooden, D. H., & Rank, D. 1989a, ApJ, 345, L59
Allamandola, L. J., Sandford, S. A., Hudgins, D. M., & Witteborn, F. C. 1995, in ASP Conf. Proc. 73, Airborne Astron. Symp. Galactic Ecosystem, ed. M. R. Haas, J. A. Davidson & E. F. Erickson (San Francisco: ASP), 23
Allamandola, L. J., Tielens, A. G. G. M., & Barker, J. R. 1985, ApJ, 290, L25
———. 1989b, ApJS, 71, 733
Beyer, T., & Swinehart, D. F. 1973, Commun. Assoc. Comput. Machin. 16, 379
Brenner, J., & Barker, J. R. 1992, ApJ, 388, L39
Cherchneff, I., & Barker, J. R. 1989, ApJ, 341, L21
Cook, D. J., Schlemmer, S., Balucani, N., Wagner, D. R., Harrison, J. A., Steiner, B., & Saykally, R. J. 1997, J. Phys. Chem., in press
Cook, D. J., Schlemmer, S., Balucani, N., Wagner, D. R., Steiner, B., & Saykally, R. J. 1996, Nature, 380 (21), 227
de Frees, D. J., Miller, M. D., Talbi, D., Pauzat, F., & Ellinger, Y. 1993, ApJ, 408, 530
Herzberg, G. H. 1968, Infrared and Raman Spectra of Polyatomic Molecules (Princeton: van Nostrand)
Hudgins, D. M., & Allamandola, L. J. 1995a, J. Phys. Chem., 99, 3033
———. 1995b, J. Phys. Chem., 99, 8978
Hudgins, D. M., Sandford, S. A., & Allamandola, L. J. 1994, J. Phys. Chem., 98, 4243
Joblin, C., Boissel, P., Léger, A., d'Hendecourt, L., & Défourneau, D. 1995, A&A, 299, 835
Joblin, C., d'Hendecourt, L., Léger, A., & Défourneau, D. 1994, A&A, 281, 923
Jochims, H. W., Rühl, E., Baumgärtel, H., Tobita, S., & Leach, S. 1994, ApJ, 420, 307
Langhoff, S. R. 1996, J. Phys. Chem., 100, 2819
Léger, A., & d'Hendecourt, L. 1989, Ann. Phys., 14, 181
Léger, A., & Puget, J. L. 1984, A&A, 137, L5
Pauzat, F., Talbi, D., Miller, M. D., de Frees, D. J., & Ellinger, Y. 1992, J. Phys. Chem., 96, 7882
Roche, P. F., Lucas, P. W., Hoare, M. G., Aitken, D. K., & Smith, C. H. 1996, MNRAS, 280, 924
Schlemmer, S., Cook, D. J., Harrison, J. A., Wurfel, B., Chapman, W., & Saykally, R. J. 1994, Science, 265, 1686
Schutte, W. A., Tielens, A. G. G. M., & Allamandola, L. J. 1993, ApJ, 415, 397
Shan, J., Suto, M., & Lee, L. C. 1991, ApJ, 383, 459
Stein, S. E., & Rabinovitch, B. S. 1973, J. Chem. Phys., 58, 2438
Szczepanski, J., Chapo, C., & Vala, M. 1993, Chem. Phys. Lett., 205, 434
Szczepanski, J., Roser, D., Personette, W., Eyring, M., Pellow, R., & Vala, M. 1992, J. Phys. Chem., 96, 7876
Szczepanski, J., & Vala, M. 1993a, ApJ, 414, 646
———. 1993b, Nature, 363, 699
Szczepanski, J., Vala, M., Talbi, D., Parisel, O., & Ellinger, Y. 1993, J. Chem. Phys., 98, 4494
Szczepanski, J., Wehlburg, C., & Vala, M. 1995, Chem. Phys. Lett., 232, 221
Vala, M., Szczepanski, J., Pauzat, F., Parisel, O., Talbi, D., & Ellinger, Y. 1994, J. Phys. Chem., 98, 9187
Williams, R. M., & Leone, S. R. 1995, ApJ, 443, 675